



NMR dynamics study of the Z-DNA binding domain of human ADAR1 bound to various DNA duplexes

Ae-Ree Lee^{a,1}, Hee-Eun Kim^{a,1}, Yeon-Mi Lee^a, Minjee Jeong^a, Kwang-Ho Choi^a, Jin-Wan Park^a, Yong-Geun Choi^a, Hee-Chul Ahn^b, Byong-Seok Choi^c, Joon-Hwa Lee^{a,*}

^a Department of Chemistry and RINS, Gyeongsang National University, Jinju, Gyeongnam 660-701, Republic of Korea

^b College of Pharmacy, Dongguk University, Goyang, Gyeonggi 410-774, Republic of Korea

^c Department of Chemistry, Korea Advanced Institute of Science and Technology, Daejeon 305-701, Republic of Korea

ARTICLE INFO

Article history:

Received 25 September 2012

Available online 15 October 2012

Keywords:

NMR

Z-DNA

Backbone dynamics

Z-DNA binding protein

DNA–protein interaction

ABSTRACT

The Z-DNA binding domain of human ADAR1 ($Z\alpha_{\text{ADAR1}}$) preferentially binds Z-DNA rather than B-DNA with high binding affinity. Here, we have carried out chemical shift perturbation and backbone dynamics studies of $Z\alpha_{\text{ADAR1}}$ in the free form and in complex with three DNA duplexes, d(CGCGCG)₂, d(CACGTG)₂, and d(CGTACG)₂. This study reveals that $Z\alpha_{\text{ADAR1}}$ initially binds to d(CGCGCG)₂ through the distinct conformation, especially in the unusually flexible $\beta 1$ –loop– $\alpha 2$ region, from the d(CGCGCG)₂–($Z\alpha_{\text{ADAR1}}$)₂ complex. This study also suggests that $Z\alpha_{\text{ADAR1}}$ exhibits a distinct conformational change during the B–Z transition of non-CG-repeat DNA duplexes with low binding affinities compared to the CG-repeat DNA duplex.

© 2012 Elsevier Inc. All rights reserved.

1. Introduction

Left-handed Z-DNA is a higher energy conformation than right-handed B-DNA [1–3]. Z-DNA forms a polymer of alternating pyrimidine–purine nucleotides, with the dC residues in the *anti*-conformation and the dG residues in the unusual *syn*-conformation [1–3]. The Z-DNA conformation can be stabilized by high salt conditions, negative supercoiling [2,3] or complex formation with Z-DNA binding proteins [4–10]. Human ADAR1, which deaminates adenine in pre-mRNA to yield inosine, consists of two Z-DNA binding domains, $Z\alpha$ and $Z\beta$ [4]. The $Z\alpha$ domain of human ADAR1 ($Z\alpha_{\text{ADAR1}}$) preferentially binds with high binding affinity to Z-DNA rather than B-DNA [11–13]. Z-DNA can also be formed in double-stranded DNA sequences that either lack alternating pyrimidine–purine base pairs or include A–T base pairs [14–16], in the following order of preference: d(CG) repeat > d(TG/AC) repeat > d(GGGC) repeat > d(TATA) repeat [17,18]. Recently, an X-ray structural study revealed that similar to CG-repeat DNA duplex, two $Z\alpha_{\text{ADAR1}}$ domains bind to each strand of non-CG-repeat DNA duplexes with 2-fold symmetry with respect to the DNA helical axis, suggesting that $Z\alpha_{\text{ADAR1}}$ recognizes Z-DNA through a common structural feature rather than by a specific sequence or by structural alternations [19]. A previous NMR study on a d(CGCGCG)₂– $Z\alpha_{\text{ADAR1}}$ complex [20] suggested an active B–Z

transition mechanism of a 6-base-paired (6-bp) DNA duplex, in which the $Z\alpha_{\text{ADAR1}}$ protein first binds to B-DNA and then converts it to left-handed Z-DNA, a conformation that is then stabilized by the additional binding of a second $Z\alpha_{\text{ADAR1}}$ molecule. $Z\alpha_{\text{ADAR1}}$ can also undergo the B–Z transition of non-CG-repeat DNA duplexes, following the sequence preference of d(CGCGCG)₂ >> d(CACGTG)₂ > d(CGTACG)₂ through multiple sequence discrimination steps [21]. However, these studies focused on the conformational change of B-DNA to Z-DNA induced by $Z\alpha_{\text{ADAR1}}$ and thus, there is little information on the structural and dynamic features of $Z\alpha_{\text{ADAR1}}$ during B–Z transition of DNA duplexes.

To investigate the structural and dynamic properties of $Z\alpha_{\text{ADAR1}}$ when it binds to DNA duplexes and induces the B–Z transition in a DNA duplex, we have performed NMR experiments on complexes between $Z\alpha_{\text{ADAR1}}$ and the three DNA duplexes: d(CGCGCG)₂ (referred to as CG6), d(CACGTG)₂ (referred to as CA6) and d(CGTACG)₂ (referred to as TA6) (see Fig. 1). The results revealed that $Z\alpha_{\text{ADAR1}}$ exhibits a distinct conformational change during the B–Z transition of non-CG-repeat DNA duplexes compared to the CG-repeat DNA duplex. This study provides valuable insights into the molecular mechanism of the sequence-specific B–Z transition induced by $Z\alpha_{\text{ADAR1}}$.

2. Materials and methods

2.1. Sample preparation

The DNA oligomers were purchased from IDT Inc. (Coralville, IA). They were purified by a reverse-phase HPLC and desalted using a

* Corresponding author. Fax: +82 55 772 1489.

E-mail address: joonhwa@gnu.ac.kr (J.-H. Lee).

¹ These authors contributed equally to this work.

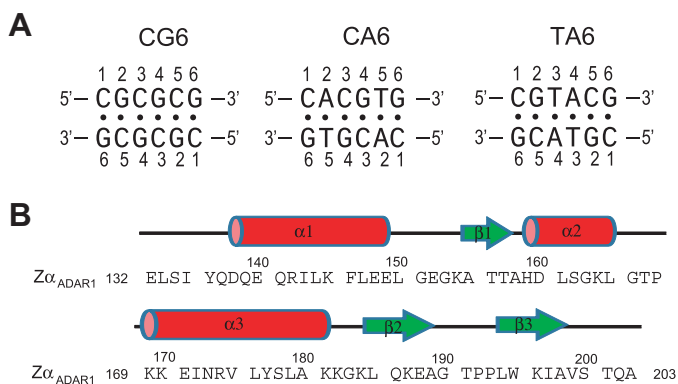


Fig. 1. (A) Sequences of the DNA duplexes and (B) $Z\alpha_{ADAR1}$. The secondary structure is drawn above the sequence.

Sephadex G-25 gel filtration column. To produce ^{15}N -labeled $Z\alpha_{ADAR1}$, BL21(DE3) bacteria expressing $Z\alpha_{ADAR1}$ were grown in M9 medium containing 1 g/L $^{15}\text{NH}_4\text{Cl}$. The expression and purification of ^{15}N -labeled $Z\alpha_{ADAR1}$ have been described in a previous report [8]. The protein concentration was measured spectroscopically using an extinction coefficient of $6970 \text{ M}^{-1} \text{ cm}^{-1}$ at 280 nm. The DNA and protein samples were dissolved in a 90% $\text{H}_2\text{O}/10\%$ D_2O NMR buffer containing 10 mM sodium phosphate (pH 8.0) and 100 mM NaCl.

2.2. NMR experiment

All NMR experiments were performed on an Agilent DD2 700 MHz spectrometer (GNU, Jinju, Korea) or a Varian 900 MHz NMR spectrometer (KIST, Seoul, Korea), equipped with a triple resonance probe. All ^1H and ^{15}N NMR spectra were obtained using complex samples that were prepared by the addition of ^{15}N -labeled $Z\alpha_{ADAR1}$ to 0.5 mM DNA samples in an NMR buffer at the indicated P/N ratio. One dimensional (1D) NMR data were processed with either the program VNMRJ (Agilent, Santa Clara, CA) or FELIX2004 (Accelrys, San Diego, CA), whereas 2D data were processed with the program NMRPipe [22] and analyzed with the program Sparky [23]. External 2,2-dimethyl-2-silapentane-5-sulfonate was used for the ^1H and ^{15}N references. The average chemical shift differences of the amide proton and nitrogen resonances between free $Z\alpha_{ADAR1}$ and $Z\alpha_{ADAR1}$ in complex with DNA were calculated with Eq. (1),

$$\Delta\delta_{\text{avg}} = \sqrt{(\Delta\delta_{\text{H}})^2 + (\Delta\delta_{\text{N}}/5.88)^2} \quad (1)$$

where $\Delta\delta_{\text{H}}$ and $\Delta\delta_{\text{N}}$ are the chemical shift differences of the amide proton and nitrogen resonances, respectively. Residue-specific rotational correlation times (τ_c) were calculated from the ^{15}N R_1 and R_2 relaxation rates using Eq. (2) [24,25]:

$$\tau_c = \frac{1}{4\pi\nu_N} \sqrt{\frac{R_2}{R_1} - 7} \quad (2)$$

3. Results and discussion

3.1. Chemical shift perturbation of $Z\alpha_{ADAR1}$ upon binding to CG6

A superposition of the $^1\text{H}/^{15}\text{N}$ -HSQC spectra of free $Z\alpha_{ADAR1}$ and $Z\alpha_{ADAR1}$ bound to CG6 at P/N ratios = 0.5 and 2.0 is shown in Supplementary Fig. S5. Resonance assignments of the amide proton spectra of free $Z\alpha_{ADAR1}$ and the $Z\alpha_{ADAR1}$ -CG6 complexes were previously reported [20]. The weighted averages of $^1\text{H}/^{15}\text{N}$ backbone chemical shift changes were determined for each residue with

Eq. (1) (Fig. 2A). At a P/N ratio = 2.0, all residues of the $\alpha 3$ helix of $Z\alpha_{ADAR1}$ undergo significant backbone chemical shift changes ($\Delta\delta_{\text{avg}} > 0.15$ ppm) upon binding to CG6 (Fig. 2A) [20]. In addition, significant chemical shift changes were observed in the $\beta 1$ - $\alpha 2$ and $\beta 2$ -loop- $\beta 3$ regions of the $Z\alpha_{ADAR1}$ -CG6 complex (Fig. 2A) [20]. These significant chemical shift perturbations suggest a direct interaction between the corresponding residues with the phosphate backbone of Z-DNA in the CG6- $(Z\alpha_{ADAR1})_2$ complex as reported in the previous crystal structural study [4]. At a P/N ratio = 0.5, the chemical shift perturbation results were very similar to those of the $Z\alpha_{ADAR1}$ -CG6 complex at P/N ratio = 2.0 reported previously [20] (Fig. 2A). This result indicates that the structural features of $Z\alpha_{ADAR1}$ in the complex with CG6 at P/N ratio = 0.5 are similar to those of $Z\alpha_{ADAR1}$ in complex with Z-DNA. However, some amide resonances, for example A158 and E171, show the slight differences in the $^1\text{H}/^{15}\text{N}$ -HSQC spectra of the $Z\alpha_{ADAR1}$ -CG6 complex at P/N ratios = 0.5 and 2.0 (Fig. 2B). These differences could be explained by the previous finding that the conformational state of $Z\alpha_{ADAR1}$ in the complex formed at $P/N \leq 1$ is a mixture of the CG6- $(Z\alpha_{ADAR1})$ and CG6- $(Z\alpha_{ADAR1})_2$ complexes [20].

3.2. Chemical shift changes of $Z\alpha_{ADAR1}$ upon binding to non CG-repeat DNA

A superposition of the $^1\text{H}/^{15}\text{N}$ -HSQC spectra of $Z\alpha_{ADAR1}$ in the free form and in a complex with CA6 at a P/N ratio = 2.0 and TA6 at a P/N ratio = 2.0 is shown in Supplementary Fig. S6. In contrast to CG6, the residues of $Z\alpha_{ADAR1}$ underwent $\Delta\delta_{\text{avg}} < 0.05$ ppm upon binding to either CA6 or TA6 when the P/N ratio = 2.0 (Fig. 3A). The same patterns in the $^1\text{H}/^{15}\text{N}$ -HSQC spectra were observed for the $Z\alpha_{ADAR1}$ -CA6 and $Z\alpha_{ADAR1}$ -TA6 complexes when the P/N ratio ≥ 1 (data not shown). These $^1\text{H}/^{15}\text{N}$ -HSQC spectra show that $Z\alpha_{ADAR1}$ complexed with CA6 or TA6 at a P/N ratio ≥ 1 exhibits a different conformational state from $Z\alpha_{ADAR1}$ complexed with CG6 (Z-DNA). A previous NMR study revealed that $Z\alpha_{ADAR1}$ has significantly lower binding affinities for CA6 and TA6 compared to CG6 [21]. Thus, at a P/N ratio ≥ 1 , both free $Z\alpha_{ADAR1}$ and $Z\alpha_{ADAR1}$ -DNA complexes could exist as the major conformational states in these mixtures. Interestingly, in the $Z\alpha_{ADAR1}$ -CA6 and $Z\alpha_{ADAR1}$ -TA6 complexes at a P/N ratio = 2, the amide resonances for five residues (173–177) of the $\alpha 3$ helix disappeared altogether (Fig. 3A), indicating that there was chemical exchange between free and DNA-bound forms of $Z\alpha_{ADAR1}$ on an intermediate NMR time scale.

To reduce the amounts of free $Z\alpha_{ADAR1}$ in the $Z\alpha_{ADAR1}$ -DNA complex samples, the $^1\text{H}/^{15}\text{N}$ -HSQC spectra of $Z\alpha_{ADAR1}$ in a complex with CA6 (P/N ratio = 0.2) and TA6 (P/N ratio = 0.2) were also acquired at 35 °C and compared to other $^1\text{H}/^{15}\text{N}$ -HSQC spectra of $Z\alpha_{ADAR1}$ (see Supplementary Fig. S6). In contrast to CG6, the residues of $Z\alpha_{ADAR1}$ underwent $\Delta\delta_{\text{avg}} < 0.2$ ppm upon binding to the CA6 and TA6 duplexes, when the P/N ratio = 0.2 (Fig. 3B). Interestingly, these $^1\text{H}/^{15}\text{N}$ -HSQC spectra of the $Z\alpha_{ADAR1}$ -CA6 and $Z\alpha_{ADAR1}$ -TA6 complexes at a P/N ratio = 0.2 are slightly different from those at a P/N ratio = 2.0 (Fig. 3A). The G153 amide signals in the $Z\alpha_{ADAR1}$ -DNA complexes at a P/N ratio = 2.0 are located at the same position as in the free $Z\alpha_{ADAR1}$ (Fig. 3B). However, when the P/N ratio = 0.2, the G153 amide protons exhibit significant chemical shift changes upon binding to CA6 and TA6 (Fig. 3B). In addition, the S178 and T191 amide protons show a larger chemical shift perturbation upon binding to CA6 and TA6 at a P/N ratio = 0.2 compared to a P/N ratio = 2.0 (Fig. 3B). The similar results were also observed in the amide signals for the loop- $\beta 1$ -loop (151–158) and the $\alpha 3$ -loop- $\beta 2$ regions (178–191) of the $Z\alpha_{ADAR1}$ -CA6 and $Z\alpha_{ADAR1}$ -TA6 complexes (Fig. 3A). The V175 residue shows no amide signal in the $Z\alpha_{ADAR1}$ -CA6 and $Z\alpha_{ADAR1}$ -TA6 complexes at a P/N ratio = 2.0; however, when the P/N ratio = 0.2, their amide resonances are observed very far from the signal of free $Z\alpha_{ADAR1}$ (close to the

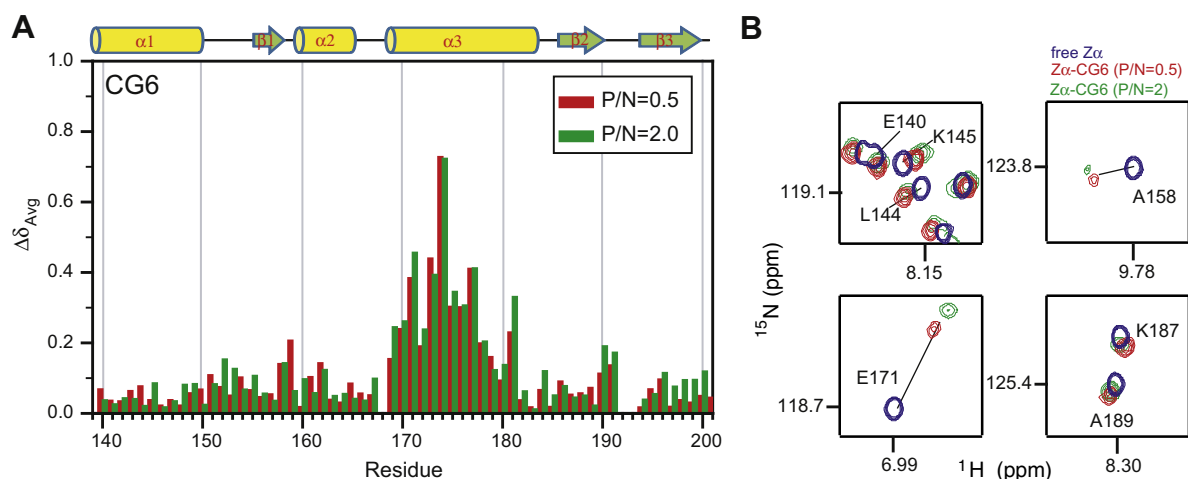


Fig. 2. (A) The weighted average of $^1\text{H}/^{15}\text{N}$ chemical shift changes ($\Delta\delta_{\text{avg}}$) of $\text{Z}\alpha_{\text{ADAR1}}$ upon binding to CG6 at P/N ratios = 0.5 (red) and 2.0 (green). (B) Comparison of the $^1\text{H}/^{15}\text{N}$ -HSQC peaks of the E140, L144, K145, A158, E171, K187, and A189 amide protons of $\text{Z}\alpha_{\text{ADAR1}}$ in the free form (blue) and in a complex with CG6 at P/N ratios = 0.5 (red) and 2.0 (green). (For interpretation of the references to color in this figure legend, the reader is referred to the web version of this article.)

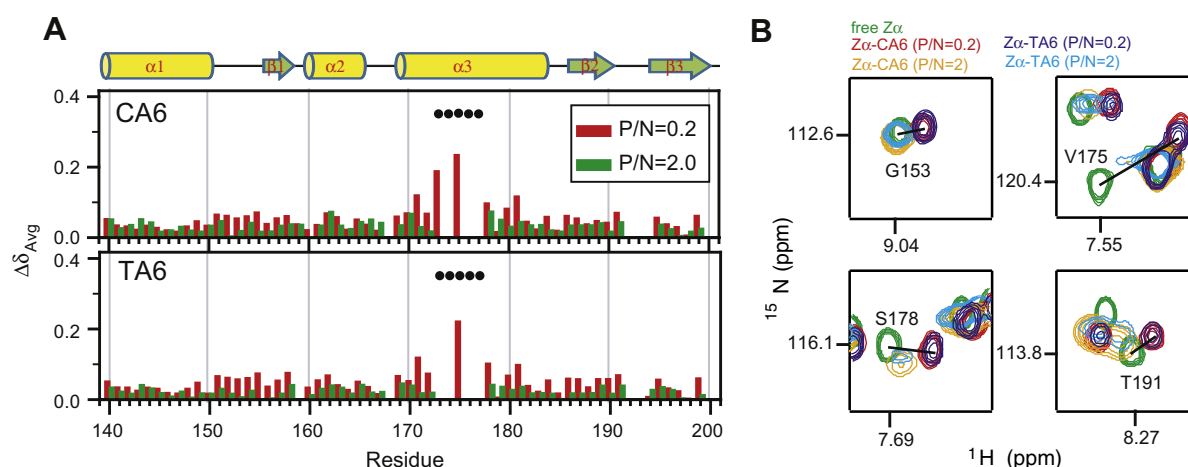


Fig. 3. (A) The weighted average of $^1\text{H}/^{15}\text{N}$ chemical shift changes ($\Delta\delta_{\text{avg}}$) of $\text{Z}\alpha_{\text{ADAR1}}$ upon binding to CA6 (upper panel) at P/N ratios = 0.2 (red) and 2.0 (green) and TA6 (lower panel) at P/N ratios = 0.5 (red) and 2.0 (green). (B) Comparison of the $^1\text{H}/^{15}\text{N}$ -HSQC peaks of the G153, V175, S178, and T191 amide protons of $\text{Z}\alpha_{\text{ADAR1}}$ in the free form (green) and in a complex with CA6 at P/N ratios = 0.2 (red) and 2.0 (orange), and with TA6 at P/N ratios = 0.2 (blue) and 2.0 (cyan). (For interpretation of the references to color in this figure legend, the reader is referred to the web version of this article.)

corresponding signal of the $\text{Z}\alpha_{\text{ADAR1}}$ –CG6 complex) (Fig. 3B). These results show that, similar to CG6, $\text{Z}\alpha_{\text{ADAR1}}$ displays a significant chemical shift perturbation upon binding to CA6 and TA6 at a P/N ratio = 0.2, but these chemical changes become smaller as the P/N ratio increases.

3.3. Relaxation rate constants of the amide protons of $\text{Z}\alpha_{\text{ADAR1}}$ in the free and in a complex with DNA

The spin–lattice (R_1) and spin–spin (R_2) relaxation rates and heteronuclear $^{15}\text{N}/^1\text{H}$ NOE for the amide protons of $\text{Z}\alpha_{\text{ADAR1}}$ in the free form and in complex with CG6 (P/N ratio = 0.5), CA6 (P/N ratio = 0.2), and TA6 (P/N ratio = 0.2) were determined at 35 °C using the standard Agilent pulse sequences. The R_1 and R_2 relaxation rates for H159 and R169 could not be determined exactly because of their very weak amide signals. In free $\text{Z}\alpha_{\text{ADAR1}}$, most amide protons, except for some amide protons in the linkers between the secondary structures and in the C-terminal region, have R_1 from 1.5 to 2.2 s^{-1} and R_2 from 7.0 to 9.0 s^{-1} (Fig. 4). In the $\text{Z}\alpha_{\text{ADAR1}}$ –CG6 complex at a P/N ratio = 0.5, all amide protons have R_1 values of 0.8–1.6 s^{-1} , which are significantly smaller than the R_1 values of the corresponding protons in the free $\text{Z}\alpha_{\text{ADAR1}}$ (Fig. 4A). However,

the R_2 values of amide protons in this complex are 3-fold larger than those in the free $\text{Z}\alpha_{\text{ADAR1}}$ (Fig. 4B). The amide protons in the linkers between the secondary structures and in the C-terminal region have larger R_1 but smaller R_2 values compared to other amide protons (Fig. 4), which are indicative of their structural flexibility. Interestingly, the R_2 values of all amide protons in the $\text{Z}\alpha_{\text{ADAR1}}$ –CA6 and $\text{Z}\alpha_{\text{ADAR1}}$ –TA6 complexes at a P/N ratio = 0.2 are between those of the free $\text{Z}\alpha_{\text{ADAR1}}$ and the $\text{Z}\alpha_{\text{ADAR1}}$ –CG6 complex (Fig. 4).

Residue-specific rotational correlation times (τ_c) were calculated from the ^{15}N R_1 and R_2 measurements on both the free $\text{Z}\alpha_{\text{ADAR1}}$ and the $\text{Z}\alpha_{\text{ADAR1}}$ –DNA complexes (Fig. 4C). In the free $\text{Z}\alpha_{\text{ADAR1}}$, the residues in the α -helices and β -sheets of the free $\text{Z}\alpha_{\text{ADAR1}}$ have an average τ_c value of 4.1 ns, while the residues in the linkers between their secondary structures have lower average τ_c values (Fig. 4C). This average τ_c value would be expected for an 8 kDa spherical protein, which is consistent with the actual molecular weight (7.5 kDa) of free $\text{Z}\alpha_{\text{ADAR1}}$. In the $\text{Z}\alpha_{\text{ADAR1}}$ –CG6 complex at a P/N = 0.5, the residues in the α -helices and β -sheets have an average τ_c value of 11.6 ns (Fig. 4C). This average τ_c value, which would be expected for a 29 kDa spherical protein, is much larger than what would be predicted for the $\text{Z}\alpha_{\text{ADAR1}}$ –CG6 (11 kDa) and ($\text{Z}\alpha_{\text{ADAR1}}$)₂–CG6 (19 kDa) complexes. This result means that the

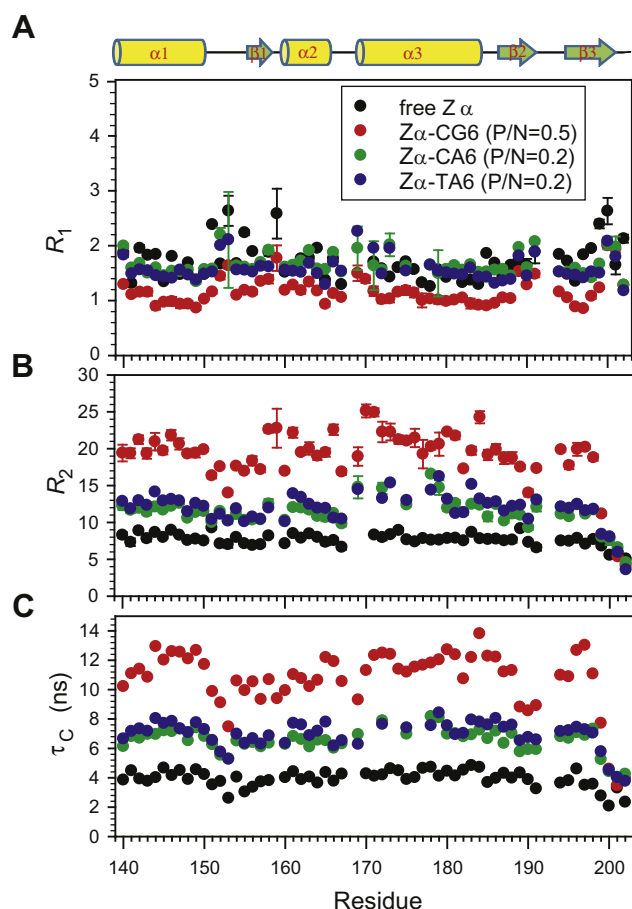


Fig. 4. The ^{15}N (A) R_1 and (B) R_2 relaxation rate constants and (C) the calculated residue-specific rotational correlation time (τ_c) as a function of residue number in the free $Z\alpha_{\text{ADAR1}}$ (black), $Z\alpha_{\text{ADAR1}}$ -CG6 ($P/N=0.5$, red), $Z\alpha_{\text{ADAR1}}$ -CA6 ($P/N=0.2$, green), and $Z\alpha_{\text{ADAR1}}$ -TA6 ($P/N=0.2$, blue) complexes. (For interpretation of the references to color in this figure legend, the reader is referred to the web version of this article.)

$Z\alpha_{\text{ADAR1}}$ -DNA complex does not have an overall spherical shape. Interestingly, the residues in the β_1 sheet and α_2 helix have average τ_c values of 10.2 and 11.1 ns, respectively, which are significantly smaller than those of other secondary structure elements (ranging from 11.7 to 12.2 ns). This result indicates that the β_1 - α_2 section of the $Z\alpha_{\text{ADAR1}}$ protein shows unusual structural flexibility in the $Z\alpha_{\text{ADAR1}}$ -CG6 complex at a $P/N = 0.5$.

The residues in the α -helices and β -sheets of the $Z\alpha_{\text{ADAR1}}$ -CA6 (P/N ratio = 0.2) and the $Z\alpha_{\text{ADAR1}}$ -TA6 (P/N ratio = 0.2) complexes have average τ_c values of 6.9 and 7.3 ns, respectively, which would be expected for 16–17 kDa spherical proteins. Similar to $Z\alpha_{\text{ADAR1}}$ -CG6 complex, in both complexes, the average τ_c value of the residues in the β_1 sheet and α_2 helix is slightly smaller than those of other secondary structural elements. The expected molecular weights could be thought of as average molecular weight values consisting of $\sim 40\%$ of the DNA-bound form (29 kDa) and $\sim 60\%$ of the free form of $Z\alpha_{\text{ADAR1}}$ (8 kDa), meaning that only 40% of $Z\alpha_{\text{ADAR1}}$ binds to CA6 or TA6, but that 60% of the proteins still remains in the free form, even though the amount of protein is 5-times higher than the amount of DNA duplex (meaning that the P/N ratio = 0.2).

3.4. Implication for the B-Z transition mechanism

The $Z\alpha_{\text{ADAR1}}$ proteins preferentially bind with high binding affinity Z-DNA rather than B-DNA [11–13]. An NMR study proposed an active B-Z transition mechanism of the DNA duplex by

$Z\alpha_{\text{ADAR1}}$, in which the $Z\alpha_{\text{ADAR1}}$ protein first binds to B-DNA and then converts it to left-handed Z-DNA, a conformation that is then stabilized by the additional binding of a second $Z\alpha_{\text{ADAR1}}$ molecule [20]. The $Z\alpha_{\text{ADAR1}}$ preferentially binds to CG6, rather than other $Z\alpha_{\text{ADAR1}}$ -CG6 complexes as the P/N ratio increased up to 1, indicating that the conformational state of $Z\alpha_{\text{ADAR1}}$ in the complex formed at a P/N ratio 1 is a mixture of CG6-($Z\alpha_{\text{ADAR1}}$) and CG6-($Z\alpha_{\text{ADAR1}}$)₂ complexes [20]. When the P/N ratio rose to ≥ 1 , free $Z\alpha_{\text{ADAR1}}$ began to bind to the $Z\alpha_{\text{ADAR1}}$ -CG6, producing the ($Z\alpha_{\text{ADAR1}}$)₂-CG6 complex, because free CG6 rarely existed under these conditions [20]. This analysis indicates that the major conformational state of $Z\alpha_{\text{ADAR1}}$ in the complex formed at a P/N ratio = 2 is the CG6-($Z\alpha_{\text{ADAR1}}$)₂ complex [20]. The difference in the intermolecular protein-DNA interactions between the CG6-($Z\alpha_{\text{ADAR1}}$) and CG6-($Z\alpha_{\text{ADAR1}}$)₂ complexes could be observed in the chemical shift perturbation data of the β_1 -loop- α_2 region (see Fig. 2). Interestingly, the average τ_c values of residues located in this region in the $Z\alpha_{\text{ADAR1}}$ -CG6 complex at a P/N ratio = 0.5 were significantly smaller than those located in other secondary structure regions (Fig. 4), indicating that the β_1 - α_2 part of $Z\alpha_{\text{ADAR1}}$ protein shows an unusual structural flexibility in the $Z\alpha_{\text{ADAR1}}$ -CG6 complex at a P/N ratio = 0.5.

The $Z\alpha_{\text{ADAR1}}$ protein can bind to both CG-repeat and non-CG-repeat DNA duplexes through a common structural feature in which two $Z\alpha$ domains bind to each strand of the double-stranded DNA with 2-fold symmetry with respect to the DNA helical axis [4,19]. Structural studies suggested that $Z\alpha_{\text{ADAR1}}$ recognizes Z-DNA through a common structural feature rather than by a specific sequence or by structural alternations [19]. However, $Z\alpha_{\text{ADAR1}}$ can induce the B-Z transition of DNA duplexes, following the sequence preference of $d(\text{CGCGCG})_2 > d(\text{CACGTG})_2 > d(\text{CGTACG})_2$ through multiple sequence discrimination steps [21]. For example, at a P/N ratio = 2.0, only 30% of the TA6 duplexes were converted to Z-DNA by $Z\alpha_{\text{ADAR1}}$, whereas most of the CG6 exhibited the Z-conformation [21]. In the case of CA6, about 60% of the DNA duplexes displayed Z-conformation at a P/N ratio = 2.0 [21]. The association constants ($K_a = [Z\alpha_{\text{ADAR1}}\text{-DNA}]/[Z\alpha_{\text{ADAR1}}][\text{DNA}]$) of the $Z\alpha_{\text{ADAR1}}$ -CA6 and $Z\alpha_{\text{ADAR1}}$ -TA6 complexes are $3.9 \times 10^3 \text{ M}^{-1}$ and $2.5 \times 10^3 \text{ M}^{-1}$, respectively, which are much smaller than that of the $Z\alpha_{\text{ADAR1}}$ -CG6 complex ($>10^7$) [21]. These values indicate that in the $Z\alpha_{\text{ADAR1}}$ -CA6 complex at a P/N ratio = 0.2 (total concentration of DNA = 0.2 mM), the relative population of the DNA-protein complex is 41%, and thus, 59% of the proteins still remains in the free form. Similarly, in the $Z\alpha_{\text{ADAR1}}$ -TA6 complex at a P/N ratio = 0.2 (total concentration of DNA = 0.2 mM), the relative populations of free protein and DNA-protein complex are 66% and 34%, respectively. These percentages are consistent with the average τ_c values of the $Z\alpha_{\text{ADAR1}}$ -CA6 and $Z\alpha_{\text{ADAR1}}$ -TA6 complexes, as determined by the backbone dynamics studies described above. Previous study reported that the equilibrium constant (K_{BZ}) between B-DNA and Z-DNA in the $Z\alpha_{\text{ADAR1}}$ -CA6 complex is about 0.4 [21], indicating that 70% of the CA6 in the complex state displayed Z-conformation (that is, 7% of overall DNA) at a P/N ratio = 0.2, and thus, 30% of the DNA remains in the B-form. In the case of the $Z\alpha_{\text{ADAR1}}$ -TA6 complex at a P/N ratio = 0.2, the K_{BZ} (= 6.3) value indicate that only 14% of the TA6 in the complex state were converted to Z-DNA (that is, 1% of overall DNA), whereas 86% of the TA6 still exhibited the B-conformation. These Z-DNA population results are consistent with the titration data of $Z\alpha_{\text{ADAR1}}$ to CA6 and TA6 by the 1D imino proton spectra in the previous study [21].

This population analysis can explain the chemical shift perturbation data showing that the residues of $Z\alpha_{\text{ADAR1}}$ underwent $\Delta\delta_{\text{avg}} < 0.2$ ppm upon binding to CA6 and TA6 when the P/N ratio = 0.2 (Fig. 3B). Interestingly, the amide protons in the loop- β_1 -loop (151–158) and the α_3 -loop- β_2 regions (178–191) show a larger chemical shift perturbation upon binding to CA6 and TA6

at a P/N ratio = 0.2 rather than a P/N ratio = 2.0 (Fig. 3B). In addition, the V175 residue shows no amide signal in either the $Z\alpha_{\text{ADAR1}}\text{-CA6}$ or the $Z\alpha_{\text{ADAR1}}\text{-TA6}$ complexes at a P/N ratio = 2.0, but when the P/N = 0.2, the amide resonances of these complexes are observed very far from the signal of the free $Z\alpha_{\text{ADAR1}}$ (close to the corresponding signal of the $Z\alpha_{\text{ADAR1}}\text{-CG6}$ complex) (Fig. 3B). Recently, it has been reported that $Z\alpha_{\text{ADAR1}}$ initially interact with 13-nucleotide DNA duplexes maintaining B-form helix via a unique conformation [26]. In this conformation, the residues of $Z\alpha_{\text{ADAR1}}$ underwent $\Delta\delta_{\text{avg}} < 0.15$ ppm upon binding to DNA duplex and the amide resonances for five residues (173–177) of the $\alpha 3$ helix disappeared altogether [26]. At a P/N ratio = 2.0, the $Z\alpha_{\text{ADAR1}}$ is thought to bind to non-CG-repeat DNA with weak binding affinity through the $\alpha 3$ helix maintaining B-form helix like initial contact conformation in the previous report [26]. Thus, we concluded that the backbone amide signals of the $Z\alpha_{\text{ADAR1}}$ were perturbed by non-CG-repeat DNA duplexes via direct DNA–protein interaction rather than conformational change of DNA duplex in the complex. In addition, the disappearance of some amide signals in the $\alpha 3$ helix indicated that they were in chemical exchange on an intermediate NMR time scale. However, at a P/N ratio = 0.2, the $Z\alpha_{\text{ADAR1}}$ binds to non-CG-repeat DNA with weak binding affinity through the $\alpha 3$ helix as well as through the loop- $\beta 1$ -loop (151–158) and the $\alpha 3$ -loop- $\beta 2$ regions (178–191). And then, the B-form helix of non-CG-repeat DNA duplexes can be converted to Z-conformation via these multiple intermolecular interactions with $Z\alpha_{\text{ADAR1}}$ proteins.

In summary, our NMR study reveals that $Z\alpha_{\text{ADAR1}}$ initially bind to CG6 through a distinct conformation, especially in the unusually flexible $\beta 1$ -loop- $\alpha 2$ region, from the $\text{CG6}-(Z\alpha_{\text{ADAR1}})_2$ complex. This study also suggests that $Z\alpha_{\text{ADAR1}}$ exhibits a distinct conformational change during the B–Z transition of non-CG-repeat DNA duplexes with low binding affinities compared to the CG-repeat DNA duplex.

Acknowledgments

This work was supported by the National Research Foundation of Korea (NRF) grants [2010-0014199, NRF-C1ABA001-2010-0020480, 2012-027750 (BRL)] funded by Korean Government (MEST). This work was also supported by a grant from Next-Generation BioGreen 21 Program (SSAC, no. PJ009041), Rural Development Administration, Korea. We thank the GNU Central Instrument Facility for performing the NMR experiments.

Appendix A. Supplementary data

Supplementary data associated with this article can be found, in the online version, at <http://dx.doi.org/10.1016/j.bbrc.2012.10.026>.

References

- [1] A. Rich, A. Nordheim, A.H. Wang, The chemistry and biology of left-handed Z-DNA, *Annu. Rev. Biochem.* 53 (1984) 791–846.
- [2] A. Herbert, A. Rich, The biology of left-handed Z-DNA, *J. Biol. Chem.* 271 (1996) 11595–11598.
- [3] A. Herbert, A. Rich, Left-handed Z-DNA: structure and function, *Genetica* 106 (1999) 37–47.
- [4] T. Schwartz, M.A. Rould, K. Lowenhaupt, A. Herbert, A. Rich, Crystal structure of the $Z\alpha$ domain of the human editing enzyme ADAR1 bound to left-handed Z-DNA, *Science* 284 (1999) 1841–1845.
- [5] T. Schwartz, J. Behlke, K. Lowenhaupt, U. Heinemann, A. Rich, Structure of the DLM-1-Z-DNA complex reveals a conserved family of Z-DNA-binding proteins, *Nat. Struct. Biol.* 8 (2001) 761–765.
- [6] S.C. Ha, N.K. Lokanath, D. Van Quyen, C.A. Wu, K. Lowenhaupt, A. Rich, Y.G. Kim, K.K. Kim, A poxvirus protein forms a complex with left-handed Z-DNA: crystal structure of a Yatapoxvirus Z bound to DNA, *Proc. Natl. Acad. Sci. USA* 101 (2004) 14367–14372.
- [7] J.D. Kahmann, D.A. Wecking, V. Putter, K. Lowenhaupt, Y.G. Kim, P. Schmieder, H. Oshkinat, A. Rich, M. Schade, The solution structure of the N-terminal domain of E3L shows a tyrosine conformation that may explain its reduced affinity to Z-DNA in vitro, *Proc. Natl. Acad. Sci. USA* 101 (2004) 2712–2717.
- [8] S.C. Ha, K. Lowenhaupt, A. Rich, Y.G. Kim, K.K. Kim, Crystal structure of a junction between B-DNA and Z-DNA reveals two extruded bases, *Nature* 437 (2005) 1183–1186.
- [9] A. Athanasiadis, D. Placido, S. Maas, B.A. Brown 2nd, K. Lowenhaupt, A. Rich, The crystal structure of the β domain of the RNA-editing enzyme ADAR1 reveals distinct conserved surfaces among Z-domains, *J. Mol. Biol.* 351 (2005) 496–507.
- [10] S.C. Ha, D. Kim, H.Y. Hwang, A. Rich, Y.G. Kim, K.K. Kim, The crystal structure of the second Z-DNA binding domain of human DAI (ZBP1) in complex with Z-DNA reveals an unusual binding mode to Z-DNA, *Proc. Natl. Acad. Sci. USA* 105 (2008) 20671–20676.
- [11] A.G. Herbert, A. Rich, A method to identify and characterize Z-DNA binding proteins using a linear oligodeoxynucleotide, *Nucl. Acids Res.* 21 (1993) 2669–2672.
- [12] A. Herbert, J. Alfken, Y.G. Kim, I.S. Mian, K. Nishikura, A. Rich, A Z-DNA binding domain present in the human editing enzyme, double-stranded RNA adenosine deaminase, *Proc. Natl. Acad. Sci. USA* 94 (1997) 8421–8426.
- [13] A. Herbert, M. Schade, K. Lowenhaupt, J. Alfken, T. Schwartz, L.S. Shlyakhtenko, Y.L. Lyubchenko, A. Rich, The $Z\alpha$ domain from human ADAR1 binds to the Z-DNA conformer of many different sequences, *Nucl. Acids Res.* 26 (1998) 3486–3493.
- [14] A.H. Wang, T. Hakoshima, G. van der Marel, J.H. van Boom, A. Rich, A-T base pairs are less stable than G-C base pairs in Z-DNA: the crystal structure of $d(m^5\text{CGTAm}^5\text{CG})$, *Cell* 37 (1984) 321–331.
- [15] M. Coll, I. Fita, J. Lloveras, J.A. Subirana, F. Bardella, T. Huynh-Dinh, J. Igolen, Structure of $d(\text{CACGTG})$, a Z-DNA hexamer containing A-T base pairs, *Nucl. Acids Res.* 16 (1988) 8695–8705.
- [16] B.F. Eichman, G.P. Schroth, B.E. Basham, P.S. Ho, The intrinsic structure and stability of out-of-alternation base pairs in Z-DNA, *Nucl. Acids Res.* 27 (1999) 543–550.
- [17] M.J. McLean, J.A. Blaho, M.W. Kilpatrick, R.D. Wells, Consecutive A T pairs can adopt a left-handed DNA structure, *Proc. Natl. Acad. Sci. USA* 83 (1986) 5884–5888.
- [18] M.J. Ellison, J. Feigon, R.J. Kelleher 3rd, A.H. Wang, J.F. Habener, A. Rich, An assessment of the Z-DNA forming potential of alternating dA-dT stretches in supercoiled plasmids, *Biochemistry* 25 (1986) 3648–3655.
- [19] S.C. Ha, J. Choi, H.Y. Hwang, A. Rich, Y.G. Kim, K.K. Kim, The structures of non-CG-repeat Z-DNAs co-crystallized with the Z-DNA-binding domain, $hZ\alpha_{\text{ADAR1}}$, *Nucl. Acids Res.* 37 (2009) 629–637.
- [20] Y.M. Kang, J. Bang, E.H. Lee, H.C. Ahn, Y.J. Seo, K.K. Kim, Y.G. Kim, B.S. Choi, J.H. Lee, NMR spectroscopic elucidation of the B–Z transition of a DNA double helix induced by the $Z\alpha$ domain of human ADAR1, *J. Am. Chem. Soc.* 131 (2009) 11485–11491.
- [21] Y.J. Seo, H.C. Ahn, E.H. Lee, J. Bang, Y.M. Kang, H.E. Kim, Y.M. Lee, K. Kim, B.S. Choi, J.H. Lee, Sequence discrimination of the $Z\alpha$ domain of human ADAR1 during B–Z transition of DNA duplexes, *FEBS Lett.* 584 (2010) 4344–4350.
- [22] F. Delaglio, S. Grzesiek, G.W. Vuister, G. Zhu, J. Pfeifer, A. Bax, NMRPipe: a multidimensional spectral processing system based on UNIX pipes, *J. Biomol. NMR* 6 (1995) 277–293.
- [23] T.D. Goddard, D.G. Kneller, SPARKY 3. University of California, San Francisco, CA, 2003.
- [24] L.E. Kay, D.A. Torchia, A. Bax, Backbone dynamics of proteins as studied by ^{15}N inverse detected heteronuclear NMR spectroscopy: application to staphylococcal nuclease, *Biochemistry* 28 (1989) 8972–8979.
- [25] L.R. Warner, K. Varga, O.F. Lange, S.L. Baker, M.C. Sousa, A. Pardi, Structure of the BamC two-domain protein obtained by Rosetta with a limited NMR data set, *J. Mol. Biol.* 411 (2011) 83–95.
- [26] Y.M. Lee, H.E. Kim, C.J. Park, A.R. Lee, H.C. Ahn, S.J. Cho, K.H. Choi, B.S. Choi, J.H. Lee, NMR study on the B–Z junction formation of DNA duplexes induced by Z-DNA binding domain of human ADAR1, *J. Am. Chem. Soc.* 134 (2012) 5276–5283.